

**Predicting the Optimal Dopant Concentration in Gadolinium Doped Ceria:  
A Kinetic Lattice Monte Carlo Approach**

Pratik P. Dholabhai: [pratik.dholabhai@asu.edu](mailto:pratik.dholabhai@asu.edu)

Materials Science & Engineering  
School for Engineering of Matter, Transport & Energy  
Arizona State University  
Tempe, Arizona 85287

Shahriar Anwar: [anwar@asu.edu](mailto:anwar@asu.edu)

Materials Science & Engineering  
School for Engineering of Matter, Transport & Energy  
Arizona State University  
Tempe, Arizona 85287

James B. Adams: [jim.adams@asu.edu](mailto:jim.adams@asu.edu)

Materials Science & Engineering  
School for Engineering of Matter, Transport & Energy  
Arizona State University  
Tempe, Arizona 85287

Peter A. Crozier: [crozier@asu.edu](mailto:crozier@asu.edu)

Materials Science & Engineering  
School for Engineering of Matter, Transport & Energy  
Arizona State University  
Tempe, Arizona 85287

Renu Sharma: [renu.sharma@nist.gov](mailto:renu.sharma@nist.gov)

Center for Nanoscale Science and Technology  
National Institute of Standards and Technology  
Gaithersburg, MD 20899

## Abstract

Gadolinium doped ceria (GDC) is a promising alternative electrolyte material for solid oxide fuel cells that offers the possibility of operation in the intermediate temperature range (773 K to 1073 K). To determine the optimal dopant concentration in GDC, we have employed a systematic approach of applying a 3-D Kinetic Lattice Monte Carlo (KLMC) model of vacancy diffusion in conjunction with previously calculated activation energies for vacancy migration in GDC as inputs. KLMC simulations were performed including the vacancy repelling effects in GDC. Increasing the dopant concentration increases the vacancy concentration, which increases the ionic conductivity. However, at higher concentrations, vacancy-vacancy repulsion impedes vacancy diffusion, and together with vacancy trapping by dopants decreases the ionic conductivity. The maximum ionic conductivity is predicted to occur at  $\approx 20\%$  to  $25\%$  mole fraction of Gd dopant. Placing Gd dopants in pairs, instead of randomly, was found to decrease the conductivity by  $\approx 50\%$ . Overall, the trends in ionic conductivity results obtained using the KLMC model developed in this work are in reasonable agreement with the available experimental data. This KLMC model can be applied to a variety of ceria based electrolyte materials for predicting the optimum dopant concentration.

## 1. Introduction

Ceria based oxides are considered one of the most promising materials for intermediate temperature (773 K to 1073 K) fuel cell applications because their high ionic conductivity facilitates the reduction in their operating temperatures, thereby eliminating several technological problems. One of the main objectives in the development of solid oxide fuel cells (SOFC) is to find electrolyte materials that exhibit improved ionic conductivity in the intermediate temperature range compared to the traditionally used yttria stabilized zirconia (YSZ). In the intermediate temperature range, oxygen ion conductivity of doped ceria is observed to be higher than YSZ [1]. Among reported results for ceria doped with different aliovalent dopants, gadolinium doped ceria (GDC) is considered to be one of the most promising solid electrolyte materials for SOFC operation in the intermediate temperature range [2,3].

As highlighted in our previous effort, ceria-doped materials have great potential for electrolyte applications in SOFC, primarily due to their high ionic conductivity [4,5,6]. Determination of the optimal dopant concentration that exhibits maximum conductivity is critical for the use of doped ceria as an electrolyte material in SOFC. For GDC, there are often inconsistent and sometimes contradictory experimental reports for the composition that exhibits the maximum conductivity. For instance, compositions with different Gd dopant concentrations such as  $\text{Ce}_{0.90}\text{Gd}_{0.10}\text{O}_{2-x}$  [3,7],  $\text{Ce}_{0.85}\text{Gd}_{0.15}\text{O}_{2-x}$  [8,9,10,11] and  $\text{Ce}_{0.80}\text{Gd}_{0.20}\text{O}_{2-x}$  [12,13,14,15,16] have been reported as optimum. A few reports also suggest that the best compositions for GDC were temperature dependent, with the optimum dopant concentration shifting towards a higher value with increasing temperature. For example, shifts from 15 % to 21 % mole fraction of the

dopant with a temperature increase from 773 K to 1073 K [11], from 20 % mole fraction to 24 % mole fraction of the dopant with a temperature increase from 973 K to 1073 K [16], and from 15 % mole fraction of the dopant below 673 K to 20 % above 673 K [14] have been reported. Steele [3] reported that a GDC sample with 10 % mole fraction of Gd exhibited the maximum conductivity, but after summarizing other authors' work, also indicated that at 773 K, the total conductivity peaks at around 25 % mole fraction of the dopant. The scatter in the optimum composition data can be attributed mainly to the divergences in sample preparation, variations in sintering temperature, and variations in the level of reduction in the samples. Moreover, the level of the purity of the ceramic sample also affects the conductivity as impure samples exhibit considerable grain boundary resistivity. SiO<sub>2</sub>, one of the predominant impurities at the grain boundary in ceria based materials, often incorporated from the precursor chemicals or the synthesis vessel during sample preparation [3,17,18], reportedly reduces the conductivity [19].

Despite of the inconsistencies in the absolute value for the optimum composition for maximum ionic conductivity in the literature, there is an agreement about the overall trend, i.e. the conductivity increases with doping concentration up to a certain value and then drops. Theoretical calculations can help us in understanding the observed trend. So far the computational studies for predicting the compositional dependence of the oxygen vacancy diffusion constant in GDC are limited to molecular dynamics simulations. Hayashi *et al.* used molecular dynamics simulations to investigate oxygen diffusion and the microscopic structure of ceria-based solid electrolytes with different dopant radii [20]. Inaba *et al.* studied oxygen diffusion in Gd-doped ceria using classical molecular dynamics simulations [21]. They reported that the diffusion constant shows a

maximum at 10 % mole fraction of Gd and decreases at higher Gd contents. They attributed the formation of Gd – vacancy – Gd clusters and long-range interactions between the oxygen vacancies to be the possible mechanisms for the decrease in the diffusion constant at higher Gd content. These molecular dynamics simulations were carried out at 1273 K, higher than the effective temperature ranges for the operation of SOFC. Hence, knowledge of various compositions of GDC showing peak conductivities at lower temperatures will provide insight in towards selecting the appropriate electrolyte materials for SOFC. Moreover, molecular dynamics simulations are performed over a very short time frame that can lead to insufficient statistical sampling of various configurations.

Since KLMC methods have proven to be useful in the investigation of oxygen diffusion in other oxides, we chose to apply this methodology to GDC [6]. KLMC models reported so far have often suffered from two limitations: i) data on dopant effects on vacancy migration limited to a single binding energy- while our calculations reveal that the dopant-vacancy interactions can be very complex, [4,5] and ii) a failure to include the effect of repulsion between the oxygen vacancies- which we find to be significant at higher concentrations [6].

Details of the development of a KLMC model for Pr-doped ceria using activation energies calculated from density functional theory +U (DFT+U) [5] to study time-dependent vacancy diffusion can be found in [6]. We have also applied first-principles (DFT+U) methodology to study oxygen vacancy migration in GDC and presented calculations of activation energy for vacancy migration along various diffusion pathways [4]. The results from these calculations are used in this work as inputs to a KLMC model

to investigate the effect of dopant concentration and temperature on ionic conductivity. Thus, the model can be used as a design tool to determine the best GDC composition for maximum ionic conductivity.

## **2. Computational Methodology**

The KLMC model requires input rates for various allowable events, such as diffusion and reactions. If these rates are known then we can accurately simulate time-dependent diffusion of various species. KLMC simulations based on a set of kinetic atomic-scale processes can describe the evolution of mesoscopic systems up to macroscopic times. In this way, we have developed a 3-D KLMC model of vacancy diffusion in GDC. This model will further enable us to calculate ionic conductivity of various GDC compositions as a function of temperature. In the current KLMC model, the material under consideration evolves as a series of independent events occur in accordance with the input rates.

The vacancy formation energy in ceria is very high ( $\approx 3$  eV); hence only a small fraction of vacancies are generated thermally. Most of the vacancies in ceria-doped materials are generated to maintain the charge balance due to the addition of aliovalent dopants. For instance, the addition of  $Gd^{+3}$  to  $CeO_2$  results in an oxygen vacancy for every two ionized dopants (since the stoichiometric vacancy to dopant ratio is 0.5). We have argued earlier [4,5] that the activation energy for vacancy migration is actually a complex average of many jump events. Hence, we have calculated activation energies of various diffusion pathways for oxygen vacancy migration in GDC for a vacancy hopping mechanism [4]. The energies from our previous work [4], as presented in Table 1, are used in the KLMC model, where every event occurs independently in accordance

with the statistically averaged activation energy corresponding to the local environment. In this article, the uncertainty in calculated energies using DFT+ $U$  is  $\approx 0.01$  eV. For GDC, the oxygen prefers a first nearest neighbor (1NN) site (Figure 1) [4], which means that many types of jump events need to be included (1NN  $\rightarrow$  2NN, 2NN  $\rightarrow$  1NN, 2NN  $\rightarrow$  2NN, 2NN  $\rightarrow$  3NN, etc.) to properly model the complexity of the diffusion process.

Details of the current methodology and a flowchart outlining the working of the KLMC model are given in an earlier paper [6]. The formalism for the calculation of vacancy diffusion coefficient followed by the calculation of ionic conductivity is explained in detail elsewhere [6]. For GDC, we used a  $10 \times 10 \times 10$  cell (consisting of 12,000 sites) built from a conventional 12-atom cubic unit cell of ceria using the theoretically optimized lattice constant of 0.5494 nm for bulk ceria [4,5]. Among these 12,000 positions, 4,000 are available for Gd dopant placement, which are assumed to be immobile. The vacancies are formed on the oxygen sublattice consisting of 8,000 sites, and are allowed to hop to adjacent sites, subject to certain constraints, such as a vacancy-vacancy repulsion factor and that the hopping mechanism is governed by an Arrhenius law [6]. The simulation cell was repeated periodically along the three axes to simulate a lattice of effectively infinite extent. The dopant and vacancy concentration were varied in order to maintain a stoichiometric vacancy to dopant ratio of 0.5, and the dopant ions were assumed to be trivalent. For each of the different dopant concentrations, ten simulations were performed, each with a different dopant distribution, with approximately 3,000,000 or more jump events for each configuration. This resulted in achieving a statistical average with a precision of  $\approx 3$  % for various dopant concentrations. The sampling did not require additional runs for each

configuration as calculated ionic conductivities converged within the order of  $\approx 3\%$  in the simulations. The simulations were performed for temperatures ranging from 673 K to 1073 K and approximately equal diffusion distances were used to calculate the final diffusion coefficients.

In the past, we have developed two separate models, a Vacancy Non-Repelling model (VNR) and a Vacancy Repelling model (VR) [6]. In the VNR model, vacancies are allowed to move anywhere in the simulation cell except into an existing vacancy site. In the VR model, the vacancies are not allowed to move adjacent (1NN, Figure 1) to any other vacancies in the simulation cell, nor into an existing vacancy site. These models were developed in order to incorporate the effect of vacancy-vacancy repulsion in ceria related materials. This effect was verified using DFT+*U* methodology, where we found that the configuration involving two vacancies separated by a distance larger than the 1NN (Figure 1) distance is energetically more stable as compared to the configuration with vacancies placed next to each other [6]. We studied two separate cases for GDC; (i) Vacancies are placed next to the dopant ions (ii) Vacancies are placed far apart from the dopant ions. For both cases, there are two possible ways to place the vacancies, (a) both vacancies are separated and (b) both vacancies are next to each other. In each case, the configuration involving two vacancies separated (possibility (a)) by a distance larger than the 1NN (Figure 1) distance is more stable by 0.32 eV and 0.15 eV respectively, as compared to the configuration with vacancies placed next to each other (possibility (b)). In this paper we only report results for KLMC-VR, which assumes that vacancies cannot move next to one-another, as explained above. Moreover, previous reports [22,23,24,25,26,27] do not include the Coulomb



interaction between the anionic species, which we have found to be important for correctly determining the optimal dopant concentration in ceria based electrolyte materials [6].

Inaba and co-workers [20,21] have reported, using molecular dynamics simulations, that an atomic arrangement with Gd – Gd pairs in GDC is more stable than the arrangement where isolated Gd atoms are distributed randomly. They reached this conclusion based on the closer agreement between experimental measurements and calculated values for the lattice parameters and the enthalpy of formation. To understand this behavior, we have investigated the effect of Gd – Gd dopant pairs in GDC using the DFT+ $U$  methodology [4,5]. All the calculations were performed for charge-neutral supercells. Similar to the reported results [20,21], we found that the atomic arrangement with Gd – Gd dopant pairs is more stable by 0.17 eV as compared to the arrangement with Gd atoms placed in isolation. In order to incorporate these results from first-principles in the KLMC model and to investigate the effect of Gd – Gd dopant pairs in maximizing the conductivity in GDC, we have developed a separate model called Vacancy-repelling Dopant Pairs (VRDP) model. In the KLMC-VRDP model, the dopants are randomly distributed in Gd – Gd pairs, with the rest of the algorithm being similar to the KLMC-VR model. In reality, only a fraction of the Gd ions will exist as pairs, depending on the processing conditions and thermal history of the sample. The KLMC-VRDP model is an approximation of the extreme case where all the dopant ions are assumed to exist in pairs, and serves as an upper-bound on the effect of pairing.

### **3. Results**

### **A. Vacancy mobility**

As reported earlier, the formation of an oxygen vacancy is found to be more favorable at the 1NN position to a  $\text{Gd}^{3+}$  ion [4], as opposed to the 2NN position (Figure 1) that was favored for a  $\text{Pr}^{3+}$  ion [5]. The vacancy migration energies calculated using DFT+ $U$  for various diffusion pathways in GDC are given in Table 1 [4], and correspond to the vacancy motion adjacent to one  $\text{Gd}^{3+}$  ion as shown in figure 1. In the presence of multiple dopant ions, a common physical scenario encountered in electrolyte materials and the current KLMC model, we use an underlying assumption that every additional Gd dopant ion in the vicinity of the migrating vacancy will have an additive effect towards the activation energy for vacancy migration. Earlier, we have tested this relationship using first-principles calculations [4,5] and explained its use in the working of the KLMC model [6]. Andersson *et al.* also reported a similar decrease in activation energy for the case where two Gd ions are next to each other [28]. Incorporating this assumption in the KLMC model, we have simulated diffusion of oxygen vacancies in the presence of multiple dopants. Under the current assumption, the estimated activation energies for multiple dopants are probably valid to about 10 meV at low to moderate concentrations, but the error may be larger at higher concentrations.

### **B. Ionic conductivity calculation using KLMC-VR model**

The primary goal of the current effort is to study various compositions of GDC within the temperature range 673 K to 1073 K and identify the compositions exhibiting peak conductivities at different temperatures. Researchers have previously studied other systems with similar methodology, but have failed to include the Coulomb interactions between the charged vacancies as mentioned in our previous effort [6].

Moreover, no literature data is available from Monte Carlo study is of various compositions of GDC. Including the effect of vacancy repelling, the simulations results in figure 2(a) correspond to the variations in ionic conductivity as a function of dopant concentration in GDC using the KLMC-VR model for temperatures ranging from 673 K to 1073 K. For temperatures ranging from 673 K to 873 K, the conductivity steadily increases as a function of dopant concentration and exhibits a broad maximum at  $\approx 20$  % mole fraction of the dopant. At higher temperatures, 973 K and 1073 K, the increase in conductivity is similar to that observed for the temperature range 673 K to 873 K, but the maximum in conductivity is shifted to a higher dopant content with a well-defined peak observed at  $\approx 25$  % mole fraction.

The decrease in ionic conductivity after reaching a maximum can be attributed to increase in binding of vacancies to dopants, and vacancy-vacancy repulsion, resulting in fewer available sites for the vacancy to migration [6].

### ***C. Ionic conductivity calculation using KLMC-VRDP model***

Simulation results presented in figure 2(b) are generated using the KLMC-VRDP model at temperatures 673 K, 873 K and, 1073 K and compared with the results obtained using the KLMC-VR model. As mentioned earlier, the VR model assumes the dopants are randomly distributed as single Gd ions, whereas the VRDP model assumes the dopants are randomly distributed as Gd – Gd pairs. For all the temperatures studied, the conductivity increases as a function of the dopant concentration and exhibits a maximum at  $\approx 20$  % mole fraction of the dopant, but the conductivity for temperatures of 873 K and 1073 K shows a broad maximum whereas that for 673 K exhibits a sharper peak. In general, the calculated magnitude of ionic conductivity is

larger when using the VR model. This is a consequence of the formation of Gd – vacancy – Gd clusters in the VRDP model, which effectively trap the vacancies and decrease the net diffusion. The Gd – vacancy – Gd cluster can be thought of as a vacancy having two 1NN Gd dopant ions. The difference in the conductivity calculated using the VR and VRDP models is smaller at lower dopant concentrations and steadily increases until it reaches a maximum at  $\approx 30$  % mole fraction of dopant content, after which the difference remains roughly constant. This could be due to the fact that above 30 % mole fraction of dopant content, even in the VR model, a significant fraction of dopant ions will form pairs and have an effect similar to that calculated by the VRDP model.

#### ***D. Comparison of the predicted optimal GDC composition with experimental data***

Experimental reports for the GDC compositions that exhibit maximum conductivity vary from 10 % [3,7], to 15 % [8,9,10,11], to 20 % [12,13,14,15,16] mole fraction of dopant. The compositions with maximum conductivity were also found to be temperature dependent [11,14,16]. For instance, at 873 K, a few of the experimental measurements [12,14,16] reported  $\approx 20$  % mole fraction of dopant content to be optimal, which is exactly the same content as predicted by the current KLMC-VR model. Figure 3 shows the various trends of increase in ionic conductivity as a function of Gd dopant concentration at 973 K for experimentally measured data. Also included in figure 3 is a plot of ionic conductivity data generated using the KLMC-VR model at 973 K. The KLMC model at this temperature predicts a maximum in ionic conductivity at  $\approx 25$  % mole fraction of Gd dopant. Most of experimental measurements report maxima at 15 % [8,9,10] and 20 % mole fraction of Gd [11,12,13,14,15,16,19]. Two other measurements

[3,7] predict  $\approx 10\%$  mole fraction of dopant content to be optimal, but the measurements were not performed for intermediate concentrations (i.e. 15% and 25% mole fraction of dopant content), so there is a possibility of the true maximum being masked. Overall, the majority of the experimental work predicts a range from 15% to 20% mole fraction of dopant content in GDC to be optimal for temperatures ranging from 673 K to 973 K. Although the calculated value of optimum composition for maximum conductivity is slightly higher than experimental numbers, the results demonstrate the root causes for the increase and subsequent decrease in conductivity after attaining the maximum.

The above results show that at higher temperatures, the KLMC-VR model predicts a slightly higher optimal dopant concentration for GDC as compared with experiment, but is in reasonable agreement at lower temperatures. The small discrepancy between the experimental and theoretical findings might be attributed to the dependence of oxygen vacancy concentration on the temperature and oxygen partial pressure. Moreover, the experimental samples are polycrystalline, and exhibit significant grain boundary resistance with increasing dopant concentration, which decreases the conductivity as compared to the current KLMC model which does not incorporate grain boundary effects. Also the discrepancy could be due to the approximation involved in estimating the migration energies in the presence of multiple dopants. The difference in the absolute magnitude of conductivity between the calculated and experimental values is approximately an order of magnitude. The reasons leading to this discrepancy require further investigation, which will be addressed in the future work, as the emphasis of the current work is on predicting the

optimal compositions of GDC. Nevertheless, the agreement between the calculated and measured values for the compositional trends is reasonable considering that all the input data for the KLMC model was generated exclusively using first-principles calculations (no experimental parameters or fitting parameters involved).

At 973 K the KLMC-VRDP model predicts  $\approx 20$  % mole fraction of dopant to be optimal (data not shown in the plot), which is in good agreement with most of the experimental measurements [11,12,13,14,15,16,19]. But a direct comparison of the data generated using the KLMC-VRDP model and experimental measurements is not appropriate as no experimental data are available that claim that all the dopants are present in the form of Gd – Gd pairs in GDC. It was reported, using MD simulations [20] carried out at 1273 K, that the oxygen diffusion coefficient of GDC shows a maximum at about 20 % mole fraction of the dopant. These calculations involved the initial placement of Gd – Gd dopant pairs in GDC similar to the KLMC-VRDP model. The result is similar to the one obtained with the current KLMC-VRDP model that predicts  $\approx 20$  % mole fraction of dopant to be optimal, but at a lower temperature (1073 K). The current simulations for GDC using KLMC-VRDP model were limited to temperatures at and below 1073 K due to its applications as an electrolyte material in SOFC. At 1273 K, we expect a slight shift to higher dopant content as compared to the reported 20 % mole fraction of dopant content [20]. At this point, further experimental information on the arrangement of dopants with respect to their placement in GDC, whether in isolation, pairs or the approximate fraction of dopants that form pairs, at specific concentrations and temperatures is needed. In future, the KLMC model can be modified to incorporate these experimental findings to enable an improved and more suitable comparison.

### ***E. Comparison with PDC***

The most favorable position for oxygen vacancy formation depends on the type of dopant ion, i.e. the 1NN position is favorable in GDC [4] and the 2NN position is favorable in PDC [5]. Depending on the preference of vacancy formation, the most favorable vacancy migration pathway in GDC is 1NN  $\rightarrow$  2NN, whereas that in PDC is 2NN  $\rightarrow$  1NN. A comparative analysis of the various migration pathways traced by oxygen vacancies in GDC and PDC provides a reasonable description of the conducting pathways and helps us identify the reasons for their respective behavior. The percent (%) differences in various migration pathways (Figure 1) traversed by vacancies during the KLMC simulations for GDC in comparison with PDC [6] at 873 K were calculated. The total mole fraction of dopant is kept fixed at 20 % mole fraction for both GDC and PDC. The analysis is performed using data for  $\approx$  3,000,000 jump events to provide a valid comparison. The net magnitude of conductivity in GDC is found to be lower than PDC [6]. In GDC, there is  $\approx$  90 % increase in the total number of 1NN  $\rightarrow$  1NN jumps, and on 11 % decrease in 1NN  $\rightarrow$  2NN and 2NN  $\rightarrow$  1NN jumps as compared to PDC. In GDC, the 2NN  $\rightarrow$  2NN jumps decreases by  $\approx$  41 % as compared to PDC. Similar analysis is conducted for other pathways. In conclusion, the conductivity in PDC is higher than in GDC owing to the higher percentage of various (more importantly 1NN  $\rightarrow$  2NN and 2NN  $\rightarrow$  1NN) migration pathways traced by the vacancies. At the end of the simulation run, a higher fraction of vacancies prefer to occupy 1NN position in GDC and 2NN position in PDC.

### ***F. Arrhenius behavior of conductivity***

Figure 4 shows values of ionic conductivity as a function of inverse temperature for low dopant concentration ( $\text{Ce}_{0.95}\text{Gd}_{0.05}\text{O}_{2-x}$ ) and for one of the most widely used composition of GDC ( $\text{Ce}_{0.80}\text{Gd}_{0.20}\text{O}_{2-x}$ ) obtained from the KLMC-VR model and experimentally measured values [8,10,11,14,16,19]. The Arrhenius type behavior of the ionic conductivity for GDC is visible with all the simulation data points for the KLMC-VR model lying on a straight line. At low dopant concentration (figure 4(a)), the simulation results at lower temperatures agree reasonably well with the experiments. As can be seen in figure 4(a), the simulated data points lie in the center of the various experimental measurements. For simulation results at higher dopant concentration (figure 4(b)), the agreement at lower temperatures is reasonable. The spread between experiment and simulations increases further at higher temperatures for both low and high dopant concentrations.

#### ***G. KLMC-VR,E model***

In the KLMC-VR model, it will be more appropriate to add the repulsion energy term explicitly. We tested this scenario using a separate model, namely the KLMC-VR,E (for Explicit) model. In this model, when a vacancy jumps to (or from) a 1NN position (Figure 1) to another vacancy, a repulsion energy term (0.30 eV) is added (or subtracted) explicitly, rather than just disallowing the jump as in the case of VR model. For temperatures from 673 K to 1073 K, the effect is at most a 3 % increase in ionic conductivity, which is negligible. Thus, the KLMC-VR is sufficient.

#### ***H. Average activation energy***

We have argued earlier [4] that the determination of the rate-limiting step for a path is complex, because it depends on the dopant concentration and their



arrangement. The input rates used for the KLMC simulations were evaluated using the DFT+*U* calculations [4] and provide a very reasonable initial assumption, but the migration energy for a complete diffusion path cannot be associated with a single migration event. It has to be averaged using a statistical model that takes into account the distinct pathways associated with a particular configuration. The average activation energy for 5 % mole fraction of the dopant in the GDC, computed using the results from KLMC-VR model, is 0.43 eV. Using DFT+*U*, we found that for  $\approx 6$  % mole fraction of the dopant, activation energy for vacancy migration of a single mobile vacancy along the most favorable path 2NN  $\rightarrow$  1NN (Figure 1) is 0.36 eV. This shows that the calculations of a single most favorable migration energy is not sufficient to correctly depict long term diffusion and that a single migration energy does not allow a fitting comparison with the experimentally measured values.

Figure 5 shows averaged activation energy for vacancy migration as a function of dopant concentration computed using the KLMC-VR model and available experimental values [3,9,11,14,19]. The calculated activation energies presented in figure 5 are computed from the slopes of similar Arrhenius plots as the one presented in figure 4. The average activation energies obtained from the KLMC simulations are significantly lower than the measured values, but the absolute ionic conductivities are in reasonable agreement with experiment from 673-1073 K (fig 4(a) and (b)).

The calculated increase in activation energy with increasing dopant concentration is also in qualitative agreement with the experimental measurements, but the effect is more pronounced for the experimental data. At higher dopant concentrations, the increase in average activation energy for migration is due to the increased likelihood of

finding two next neighbors Gd – Gd pairs near an oxygen vacancy, where a higher energy is needed to overcome these barriers. Any further increase in the Gd ions can eventually trap the vacancy and form a bottleneck for diffusion.

The differences between theory and experiment may be partly due to limitations in the DFT data used as input, the assumptions involved in the KLMC model for multiple dopants, and grain boundary diffusion effects that are not included in the model.

#### **4. Conclusions**

KLMC simulations have been conducted to predict the optimal dopant composition for GDC that exhibits maximum ionic conductivity. As an input to the KLMC model, we have used the activation energies for vacancy migration along distinct diffusion pathways calculated using DFT+*U*. Applying the KLMC-VR model for the temperature ranges 673 K to 1073 K,  $\approx 20\%$  to  $25\%$  mole fraction of dopant content is found to be optimal for achieving maximum ionic conductivity in GDC. Considering the approximations involved, as discussed in detail in our previous paper [6], the calculated results are in reasonable agreement with most experimental data finding a maximum at  $\approx 15\%$  mole fraction to  $\approx 20\%$  mole fraction of the dopant. The conductivity initially increases due to the increased number of vacancies, required for charge balance, but later decreases due to decreasing vacancy mobility (caused by vacancy-vacancy repulsion and vacancy-dopant binding). We also present an alternative KLMC-VRDP model, which assumes that all the dopants are placed in Gd – Gd pairs. The KLMC-VRDP model results in slightly lower conductivities, and shifts the peak to somewhat lower dopant concentrations. Based on the reasonable agreement with experimental measurements, the KLMC model in conjunction with first-principles calculations can be

used as a design tool to predict the optimal dopant concentration in ceria related materials for electrolyte applications.

The KLMC code developed for this project will be available for download in the near future from: <http://enpub.fulton.asu.edu/cms/>

### **Acknowledgements**

This paper is based upon the work supported by the Department of Energy under the Grant No. DE-PS02-06ER06-17. The authors gratefully acknowledge the Fulton High Performance Computing Initiative (HPCI) at the Arizona State University for the computational resources.

## References

- [1] Mogensen M, Sammes N, Tompsett G 2000 Physical, chemical and electrochemical properties of pure and doped ceria *Solid State Ionics* **129** 63
- [2] Steele B, Heinzl A 2001 Materials for fuel-cell technologies *Nature* **414** 345
- [3] Steele B 2000 Appraisal of  $\text{Ce}_{1-y}\text{Gd}_y\text{O}_{2-y/2}$  electrolytes for IT-SOFC operation at 500°C *Solid State Ionics* **129** 95
- [4] Dholabhai P, Adams J, Crozier P, Sharma R 2010 A density functional study of defect migration in gadolinium doped ceria *Phys. Chem. Chem. Phys.* **12** 7904
- [5] Dholabhai P, Adams J, Crozier P, Sharma R 2010 Oxygen vacancy migration in ceria and Pr-doped ceria: A DFT+U study *J. Chem. Phys.* **132** 094104
- [6] Dholabhai P, Anwar S, Adams J, Crozier P, Sharma R 2011 Kinetic lattice Monte Carlo model for oxygen vacancy diffusion in praseodymium doped ceria: Applications to materials design *J. Solid State Chem.* **184** 811
- [7] Chourashiya M, Patil J, Pawar S, Jadhav L 2008 Studies on structural, morphological and electrical properties of  $\text{Ce}_{1-x}\text{Gd}_x\text{O}_{2-x/2}$  *Mat. Chem. Phys.* **109** 39
- [8] Zha S, Xia C, Meng G 2003 Effect of Gd (Sm) doping on properties of ceria electrolyte for solid oxide fuel cells *Journal of Power Sources* **115** 44
- [9] Wang F, Wan B, Cheng S 2005 Study on  $\text{Gd}^{3+}$  and  $\text{Sm}^{3+}$  co-doped ceria-based electrolytes *J. Solid State Electrochem.* **9** 168
- [10] Guan X, Zhou H, Liu Z, Wang Y, Zhang J 2008 High performance  $\text{Gd}^{3+}$  and  $\text{Y}^{3+}$  co-doped ceria-based electrolytes for intermediate temperature solid oxide fuel cells *Mat. Res. Bull.* **43** 1046

- [11] Ivanov V, Khrustov V, Kotov Y, Medvedev A, Murzakaev A, Shkerin S, Nikonov A 2007 *J. Eur. Cera. Soc.*, 2007 Conductivity and structure features of  $Ce_{1-x}Gd_xO_{2-\delta}$  solid electrolytes fabricated by compaction and sintering of weakly agglomerated nanopowders **27** 1041
- [12] Kudo T, Obayashi H 1976 Mixed Electrical Conduction in the Fluorite-Type  $Ce_{1-x}Gd_xO_{2-x/2}$  *J. Electrochem. Soc.* **123** 415
- [13] Peng C, Zhang Z 2007 Nitrate–citrate combustion synthesis of  $Ce_{1-x}Gd_xO_{2-x/2}$  powder and its characterization *Ceramics Inter.* **33** 1133
- [14] Tianshu Z, Hing P, Huang H, Kilner J 2002 Ionic conductivity in the  $CeO_2$ – $Gd_2O_3$  system ( $0.05 \leq Gd/Ce \leq 0.4$ ) prepared by oxalate coprecipitation *J Solid State Ionics* **148** 567
- [15] Zhang T, Ma J, Kong L, Chan S, Kilner J 2004 Aging behavior and ionic conductivity of ceria-based ceramics: a comparative study *Solid State Ionics* **170** 209
- [16] Fu Y, Chang Y, Wen S 2006 Microwave-induced combustion synthesis and electrical conductivity of  $Ce_{1-x}Gd_xO_{2-x/2}$  ceramics *Mat. Res. Bull.* **41** 2260
- [17] Vn Dijk T, Buggaaf A 1981 Grain Boundary Effects on Ionic Conductivity in Ceramic  $Gd_xZr_{1-x}O_{2-x/2}$  Solid Solutions *Phys. Stat. Sol. (a)* **63** 229
- [18] Gerhardt R, Nowick A 1986 Grain-Boundary Effect in Ceria Doped with Trivalent Cations: I, Electrical Measurements *J. Am. Ceram. Soc.* **69** 641
- [19] Zhang T, Ma J, Cheng J, Chan S 2006 Ionic conductivity of high-purity Gd-doped ceria solid solutions *Mat. Res. Bull.* **41** 563
- [20] Hayashi H, Sagawa R, Inaba H, Kawamura K 2000 *Solid State Ionics* **131** 281
- [21] Inaba H, Sagawa R, Hayashi H, Kawamura K 1999 *Solid State Ionics* **122** 95

- [22] Pornprasertsuk R, Ramanarayanan P, Musgrave C, Prinz F 2005 Predicting ionic conductivity of solid oxide fuel cell electrolyte from first principles *J. Appl. Phys.* **98** 103513
- [23] Pornprasertsuk R, Holme T, Prinz F 2009 Kinetic Monte Carlo Simulations of Solid Oxide Fuel Cell *J Electro. Soc.* **156** B1406
- [24] Krishnamurthy R, Yoon Y, Srolovitz D, Car R 2004 Oxygen Diffusion in Yttria-Stabilized Zirconia: A New Simulation Model *J. Am. Ceram. Soc.* **87** 1821
- [25] Murray A, Murch G, Catlow C 1986 A new hybrid scheme of computer simulation based on Hades and Monte Carlo: Application to ionic conductivity in  $Y^{3+}$  doped  $CeO_2$  *Solid State Ionics* **18** 196
- [26] Adler S, Smith J, Reimer J 1993 Dynamic Monte Carlo simulation of spin-lattice relaxation of quadrupolar nuclei in solids. Oxygen-17 in yttria-doped ceria *J. Chem. Phys.* **98** 7613
- [27] Adler S, Smith J 1993 Effects of long-range forces on oxygen transport in yttria-doped ceria: simulation and theory *J. Chem. Soc. Farad. Trans.* **89** 3123
- [28] Andersson D, Simak S, Skorodumova N, Abrikosov I, Johansson B 2006 Optimization of ionic conductivity in doped ceria *PNAS* **103** 3518

Table 1. Activation energies ( $E_a$ ) for oxygen vacancy migration along various diffusion pathways in GDC calculated using DFT+ $U$ . The nearest neighbor positions are given with respect to the Gd ion as given in figure 1.

Migration pathway	$E_a$ (eV)	Migration pathway	$E_a$ (eV)	Migration pathway	$E_a$ (eV)
1NN $\rightarrow$ 1NN	0.59	2NN $\rightarrow$ 1NN	0.36	3NN $\rightarrow$ 1NN	2.46
1NN $\rightarrow$ 2NN	0.50	2NN $\rightarrow$ 2NN	0.48	3NN $\rightarrow$ 2NN	0.46
1NN $\rightarrow$ 3NN	2.61	2NN $\rightarrow$ 3NN	0.49	3NN $\rightarrow$ 3NN	0.47

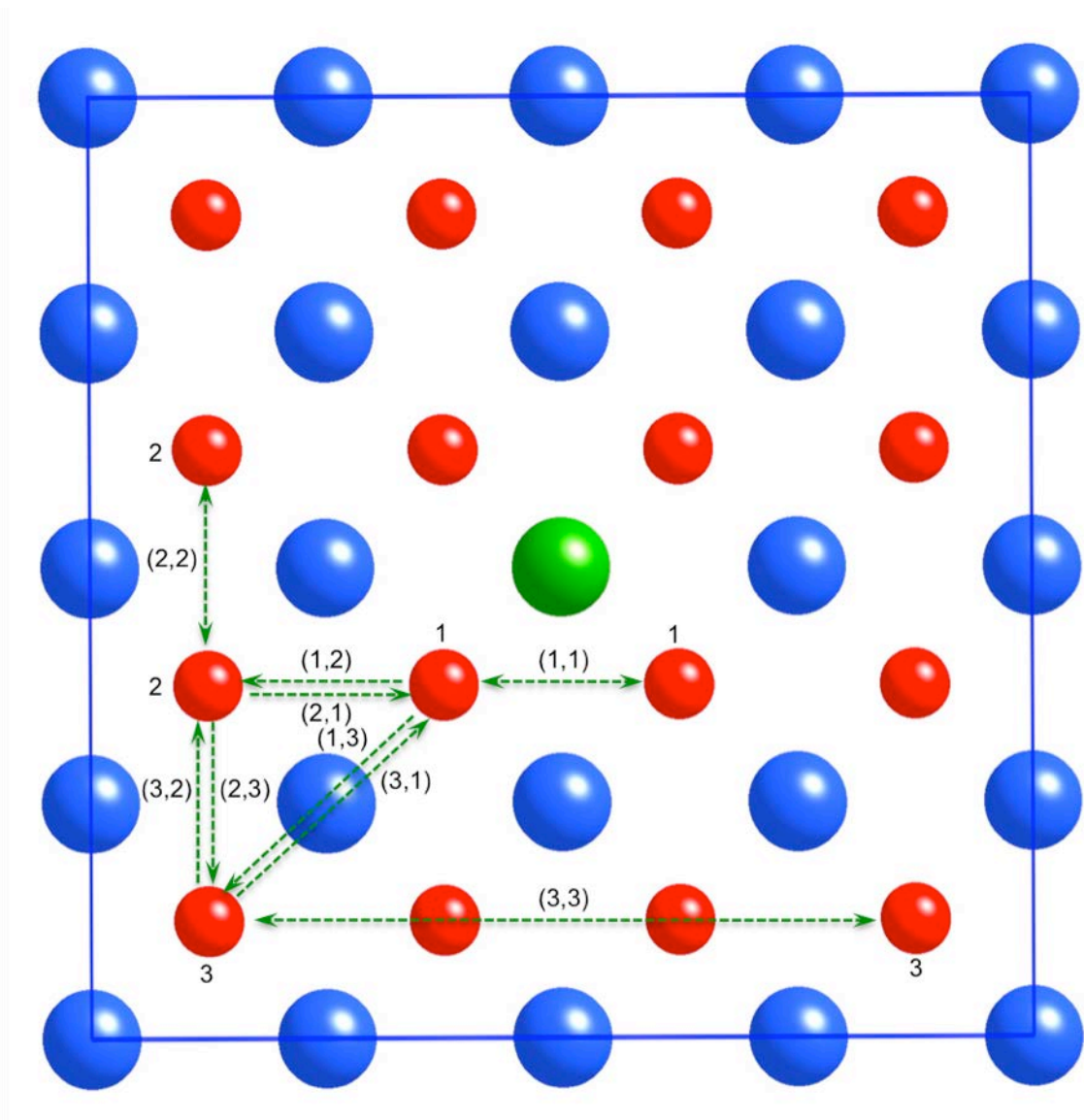


Figure 1. Top view of a  $2 \times 2 \times 2$  GDC supercell. The blue, green and red balls represent Ce, Gd and O ions, respectively. Numbers 1, 2 and 3 represent 1NN, 2NN and 3NN oxygen ions with respect to the Gd ion, respectively. (X, Y) represents an oxygen ion jump from XNN to YNN. Gd ion closer to the migrating vacancy is only shown. Corresponding energies are given in table 1.



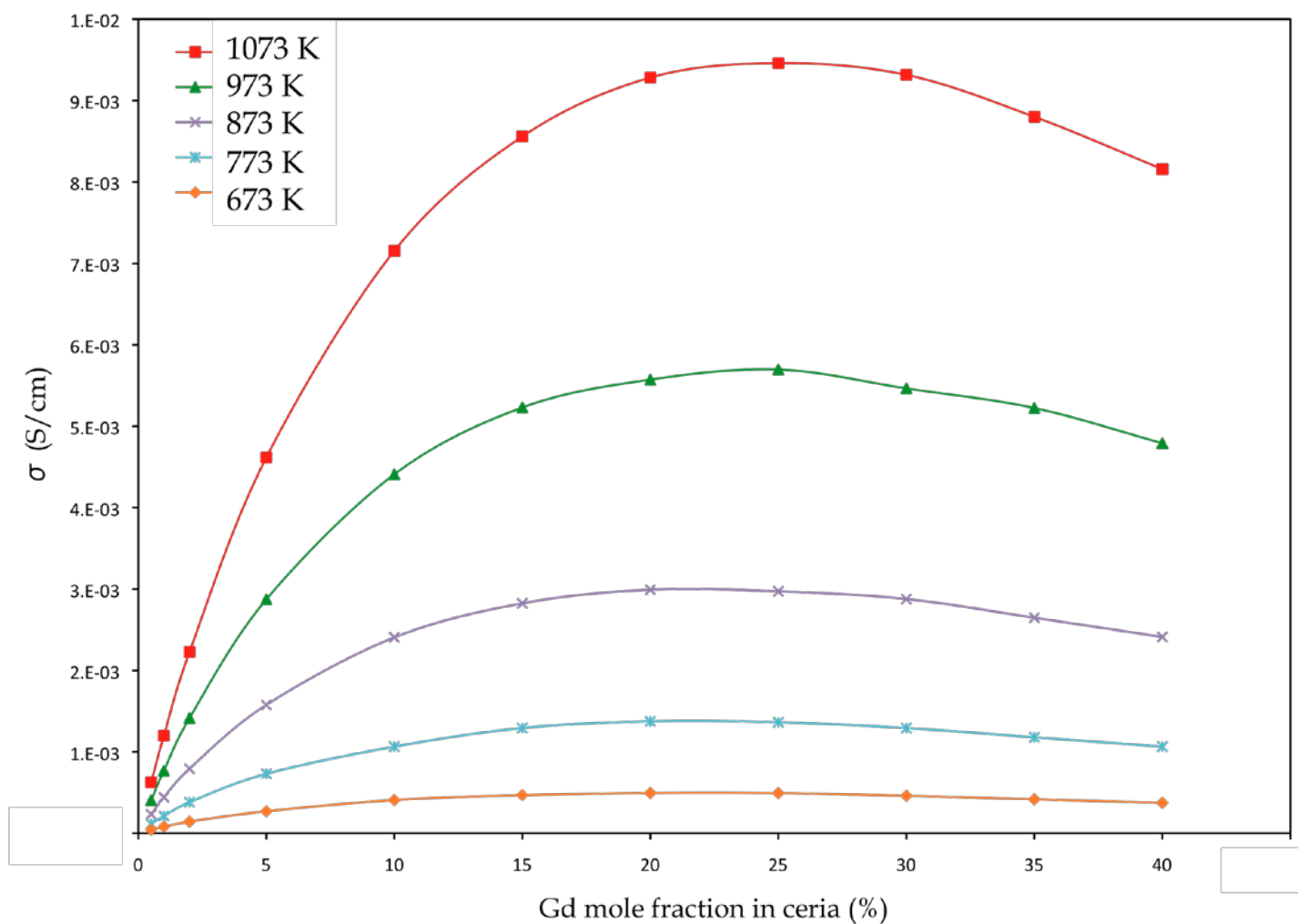


Figure 2(a). Calculated ionic conductivity in GDC as a function of dopant content generated using KLMC-VR model for temperature ranging from 673 K – 1073 K.

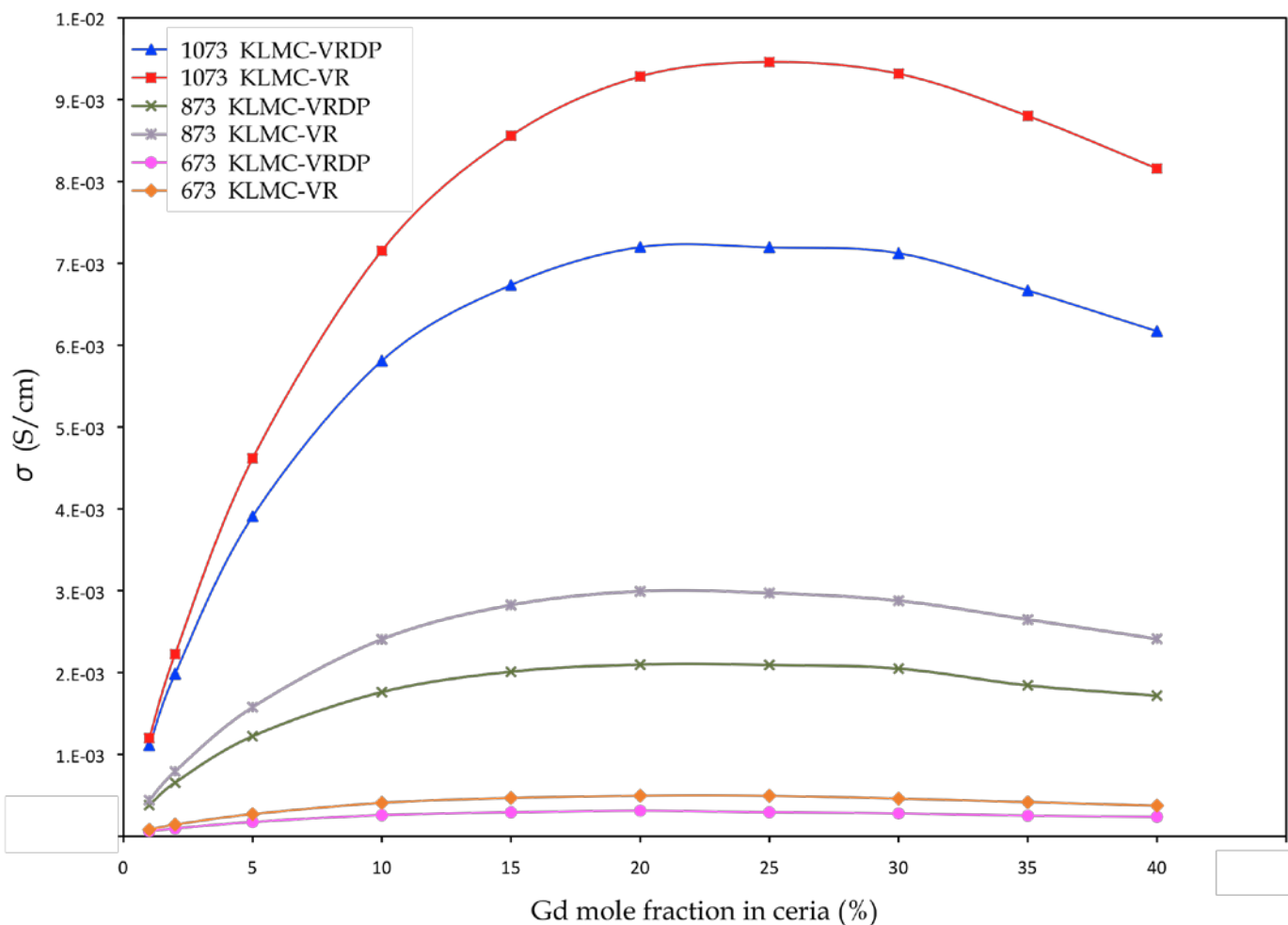


Figure 2(b). Calculated ionic conductivity in GDC as a function of dopant content generated using KLMC-VRDP model for temperatures 673 K, 873 K and 1073 K. Data generated using KLMC-VR model for the same temperatures are also shown for comparison.

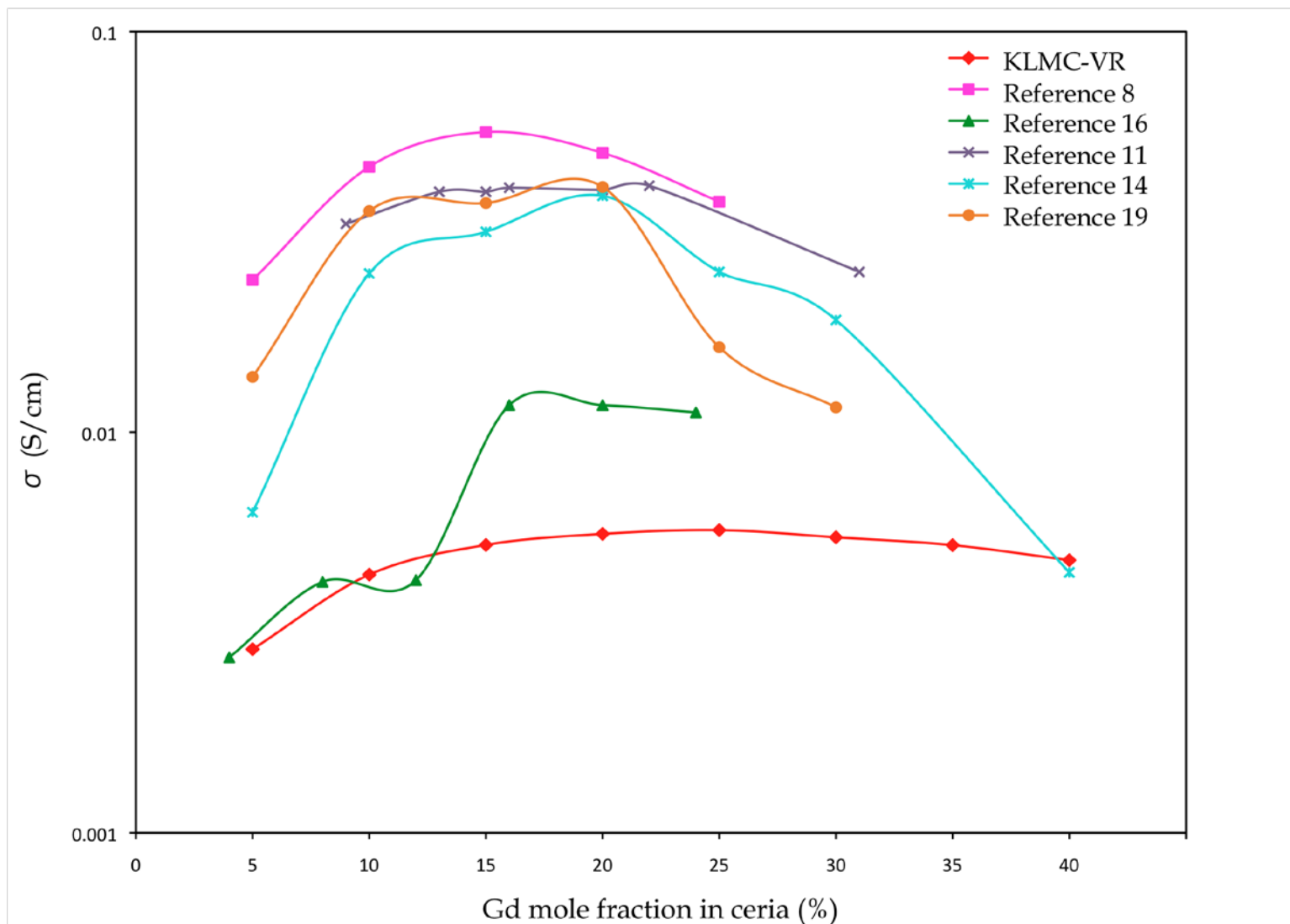


Figure 3. Calculated (using KLMC-VR model) and measured ionic conductivity in GDC as a function of dopant content at 973 K.

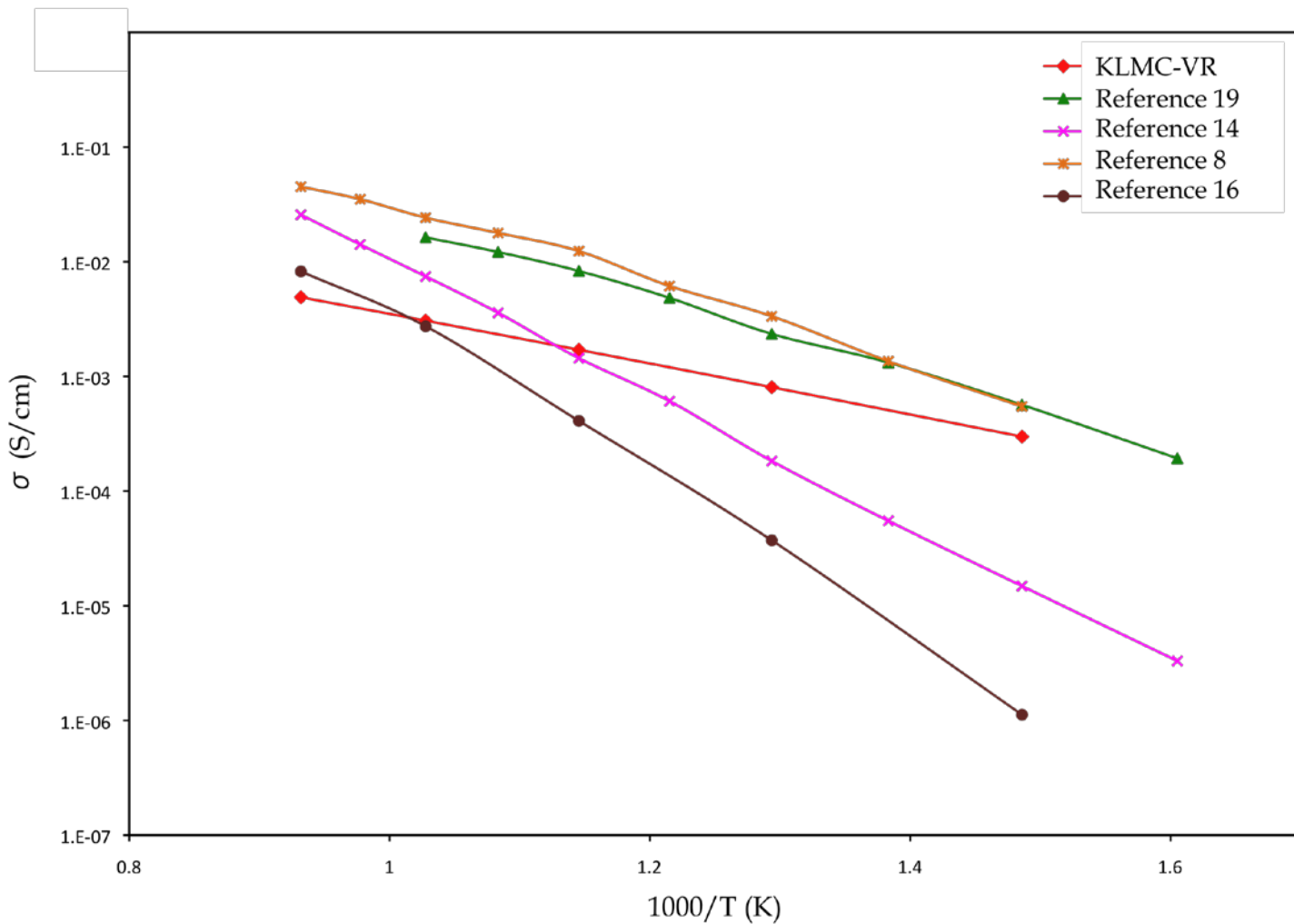


Figure 4(a). Arrhenius plot of ionic conductivity of  $\text{Ce}_{0.95}\text{Gd}_{0.05}\text{O}_{2-x}$  as a function of temperature calculated using the KLMC-VR model and compared with the available experimental data. For reference 16, the data is plotted for  $\text{Ce}_{0.96}\text{Gd}_{0.04}\text{O}_{2-x}$ .

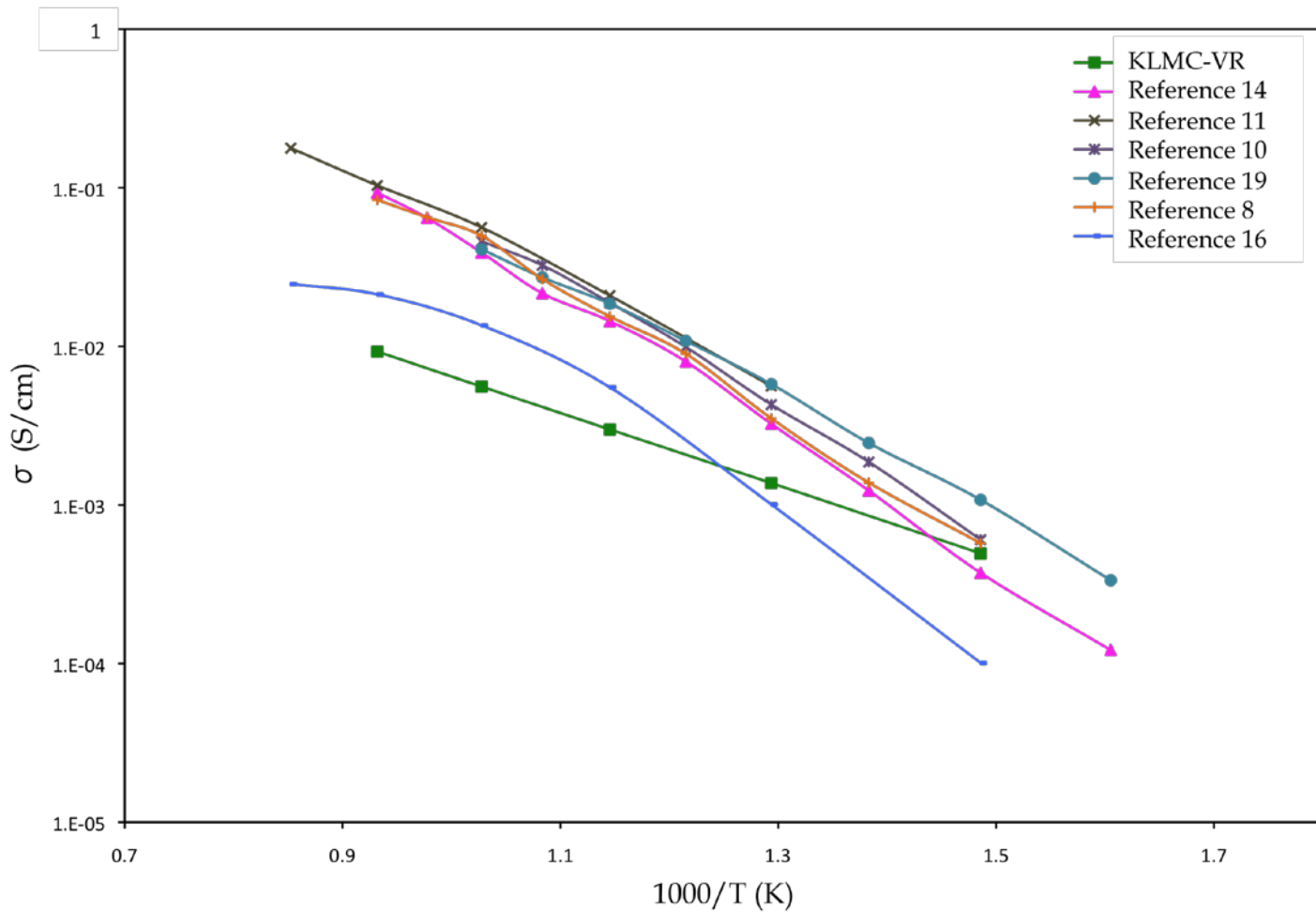


Figure 4(b). Arrhenius plot of ionic conductivity of  $\text{Ce}_{0.80}\text{Gd}_{0.20}\text{O}_{2-x}$  as a function of temperature calculated using the KLMC-VR model and compared with the available experimental data.

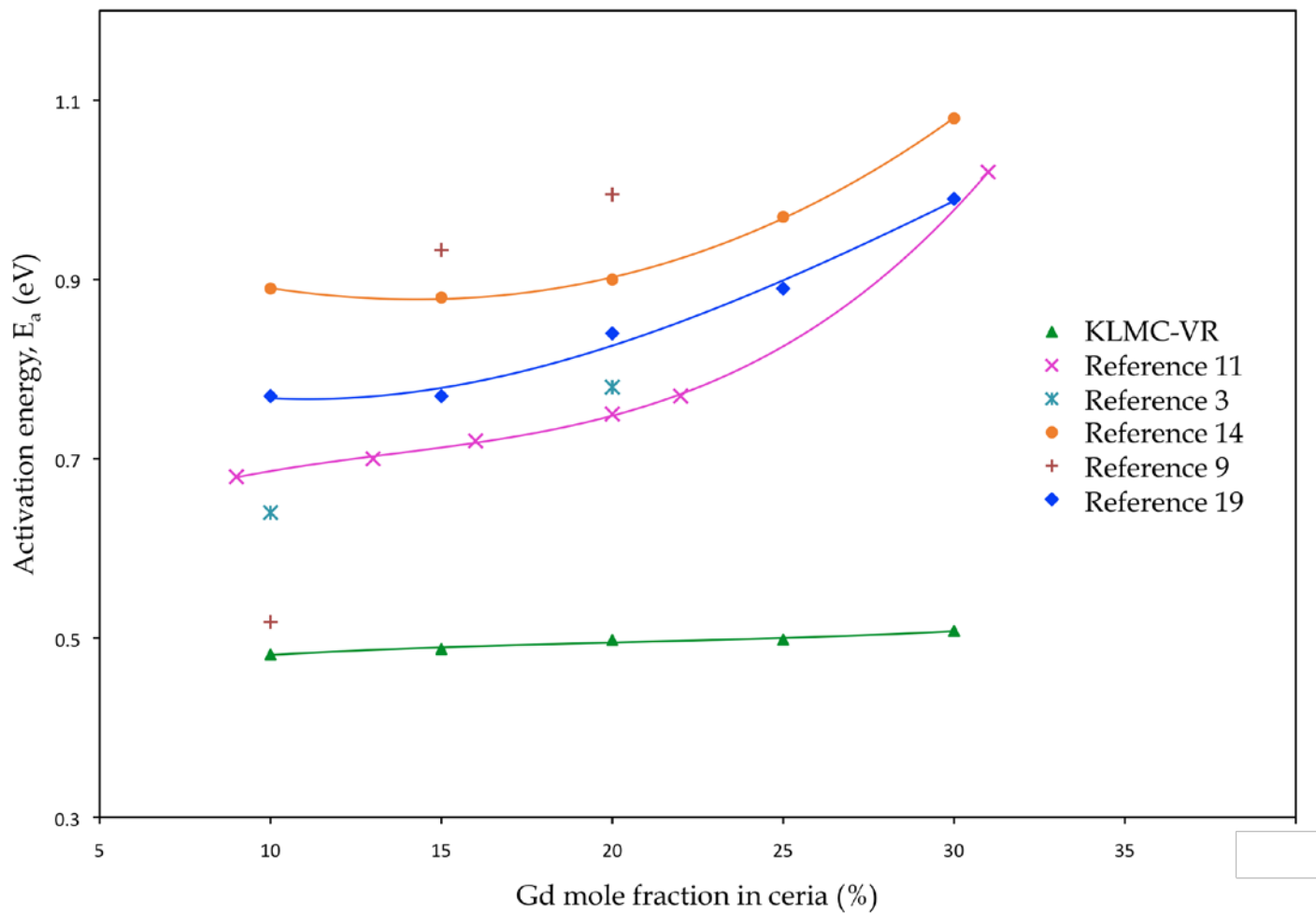


Figure 5. Average activation energy as a function of dopant content for GDC calculated using the KLMC-VR model and compared with the available experimental data.